



# Influence of Grit Blasting on the Roughness and the Bond Strength of Detonation Sprayed Coating

D. Sen, Naveen M. Chavan, D.S. Rao, and G. Sundararajan

(Submitted August 5, 2009; in revised form November 27, 2009)

The process of roughening the surfaces by grit blasting prior to coating them using thermal spray techniques is very important to obtain consistently high tensile bond strength between the coating and the substrate. The available literature on the influence of grit-blasting parameters in the case of detonation spray or HVOF coatings is quite limited. The present study aims to study the influence of grit-blasting pressure and alumina grit size on the roughening of the mild steel substrate, the resulting effect on the roughness of Cu, Al<sub>2</sub>O<sub>3</sub>, and WC-12Co coatings deposited by detonation spray coating and also on the tensile bond strengths of these coatings. Toward the above purpose, the velocity of the alumina grits have been experimentally measured using a high-speed imaging system and the tensile bond strength of the coatings have been experimentally obtained using the pin type test. The results from the above experiments point to the importance of not only the roughness of the grit-blasted mild steel substrate but also the roughness of the coatings subsequently deposited in determining the magnitude of the bond strength.

**Keywords** alumina grit velocity, coating roughness, detonation spray coatings, grit blasting, substrate roughness, tensile bond strength of coatings

## 1. Introduction

Thermal spray coatings, especially those obtained using high velocity oxy-fuel (HVOF) or detonation spray coating (DSC) techniques, are widely used to provide wear resistance to engineering structures and components operating in hostile environment. In the HVOF/DSC techniques, powder particles are heated to high temperatures and also accelerated to high velocities and then allowed to repeatedly impact the component surface to form thick coatings. A unique aspect of these HVOF/DSC coatings is that their adhesion/bonding with the substrate is largely mechanical in nature since the powder particles are invariably heated to temperatures well below their melting point. This is especially true in the case of cermet and ceramic coatings. To improve the coating-substrate adhesion, the component surfaces are always grit blasted to roughen them, prior to the coating process. Al<sub>2</sub>O<sub>3</sub> is the most widely used grit material and commercial grit-blasting machines are readily available to grit blast and roughen even components with complex geometries.

D. Sen, Naveen M. Chavan, D.S. Rao, and G. Sundararajan, International Advanced Research Centre for Powder Metallurgy and New Materials, Hyderabad, India. Contact e-mails: gsundar@arci.res.in and director@arci.res.in.

A large number of process and other variables like the grit material and size, blasting pressure and time, stand-off distance, blasting angle and the hardness of the component/surface being grit blasted determine the magnitude and nature of roughening of the surface. Thus, to obtain a consistently high quality HVOF/DSC coating with a consistently high value for the coating-substrate adhesion/bond strength, the grit-blasting process needs to be adequately controlled and more importantly, the process parameters require optimization.

A perusal of the literature indicates that considerable work has been carried out on the evaluation of the grit-blasting parameters on the roughening of the substrate per se (Ref 1-8) and also on the subsequent effect of such a roughening on the coating-substrate bond strength (Ref 1, 2, 5, 9-11). However, the bulk of the data and analyses pertains to air plasma spray coatings (Ref 1, 2, 5, 11) and the results from such studies may not be directly applicable to HVOF/DSC coatings wherein the powder particle velocities are considerably higher but their temperatures are substantially lower. Further, during the air plasma spray (APS) coating process, the powder feed stock becomes molten (irrespective of whether it is metallic or ceramic) and thus the molten particle impacts the substrate to form the coating. In contrast, in the HVOF/DSC systems, the powder particles are still solid (except in the case of low melting metallic particles) as they impact the substrate. Due to this difference, HVOF/DSC coatings usually exhibit compressive residual stress in contrast to a tensile residual stress obtained in APS coatings. Given the above differences, it is expected that the bond strength results obtained using APS systems cannot be directly applied to coatings obtained using HVOF/DSC systems.

However, the literature data obtained on the influence of grit-blasting parameters on roughening of the substrate surface are obviously relevant to HVOF/DSC coating systems as well. The surface roughness, defined in terms of parameter  $R_a$ , generally increases with increasing grit size (Ref 2, 3, 6-8). On the other hand, influence of blasting distance, blasting angle, and blast pressure on surface roughness is less clear with various investigators reporting marginal or no effect (Ref 1-5, 8, 12). Another important parameter related to grit blasting which can have a substantial effect on bond strength of the coating with the substrate is the extent to which grit residue is retained on the blasted surface prior to coating. It has been observed that the area fraction of grit residue on the blasted surface increases with increasing blasting pressure and angle (Ref 3, 4) and increasing grit size (Ref 3). Lastly, the influence of grit-blasting parameters on the bond strength has been studied by numerous investigators (Ref 1, 2, 5, 9-11). In the case of air plasma spray coatings, Bahbou et al. (Ref 1) examined the influence of blasting angle on bond strength of Triballoy 800 on Ti-6Al-4V substrate and noted that increasing the blasting angle from 45° to 90°, continuously increased the surface roughness ( $R_a$ ) and also the adhesion strength. In contrast, Day et al. (Ref 2) and Amada and Hirose (Ref 5) did not observe any correlation between bond strength and surface roughness in the case of air plasma spray coatings of Co-based alloy and  $Al_2O_3$ , respectively. In contrast, Hofinger et al. (Ref 11) observed that increasing the surface roughness increased the interface fracture energy of the air plasma sprayed NiCrAlY coatings. Finally, the very limited data available on HVOF coatings indicate that a higher surface roughness, either caused by increasing blast pressure (Ref 9) or by increasing grit size (Ref 10), results in an increase in bond strength.

The above literature review clearly indicates that in the case of HVOF/DSC coatings, the available data on the influence of shot blasting on the roughness of the substrate and on the bond strength of the coating subsequently deposited is extremely limited. One reason for such a scenario is that HVOF/DSC coatings exhibit bond strength considerably higher than that of air plasma spray coatings and as a result, the commonly used pull-off adherence test carried out using epoxy tape and as per ASTM Standards (ASTM C633) is inadequate. This is so because even the best available epoxy tapes cannot measure bond strength higher than 70 MPa while many of the HVOF/DSC coatings exhibit bond strengths which are even higher. Another drawback with the earlier works is that they correlate surface roughness and coating bond strength with process parameters like grit size and blast pressure. However, a more fundamental parameter is the grit velocity which is a strong function of grit size and blast pressure. Thus, correlation of substrate roughness with grit velocity is likely to provide a better understanding of the physics behind the shot blasting process. Lastly, the limited data available on HVOF/DSC coatings are restricted to WC-Co coatings and no data are available on either ceramic or metallic coatings.

Given the above scenario, the objective of the present work is to study the influence of grit-blasting parameters

like grit size and blasting pressure on the surface roughness of the mild steel substrate surface and also on the coating-substrate bond strength in the case of Cu, WC-Co, and  $Al_2O_3$  coatings formed on the above substrate utilizing the detonation spray coating technique. In addition, the grit velocity has been measured and the bond strength has been estimated using the pin type test described in the next section.

## 2. Experimental Details

### 2.1 Grit Blasting

The grit blasting was carried out using a suction type grit-blasting machine (MECSHOT, India). Details regarding the parameters and the grits used for grit blasting are provided in Table 1. Alumina powders of 40 and 60 mesh size were used as the grit. Typical SEM micrographs of the alumina grits are presented in Fig. 1. The average particle sizes corresponding to the above mesh sizes were determined using an image analyzer in conjunction with SEM. The software evaluated the size of individual grit particle by equating its area (as observed in SEM) with an equivalent circle of same area and assuming particle size as the diameter of the equivalent circle and repeated this procedure for more than 100 grit particles and arrived at the average particle size as  $427 \pm 40$  and  $231 \pm 47 \mu\text{m}$ , respectively, for the alumina grit of mesh sizes 40 and 60, respectively.

During the grit-blasting experiments, the grit velocity was measured using a high speed imaging system (Spray Watch 2i, Oseir Ltd., Finland) which included a diode laser based system (Hi Watch) used for illuminating the grit particles while in flight (Ref 13). The above system emits three pulses at predetermined time intervals and thereby determines the grit location over two time durations to estimate its velocity. The velocities of thousands of grits were measured in this manner. The scatter in the measured grit velocities was  $\pm 20\%$  around the average value of the velocities. However, only the average grit velocity is being reported in this study.

### 2.2 Coating Deposition

Three types of coatings, namely Cu, WC-Co, and  $Al_2O_3$  were deposited using the detonation spray coating system

**Table 1** Grit-blasting parameters

S. no.	Blasting parameters	
1	Blasting pressure, kPa	10.35, 13.8 & 20.7
2	Blasting media	Gray alumina
3.	Grit size number and average particle size	40 mesh ( $427 \pm 40 \mu\text{m}$ ) 60 mesh ( $231 \pm 47 \mu\text{m}$ )
4	Standoff distance	195 mm
5	Blasting angle	90°
6	Blasting time	2 min(a)

(a) Optimized value

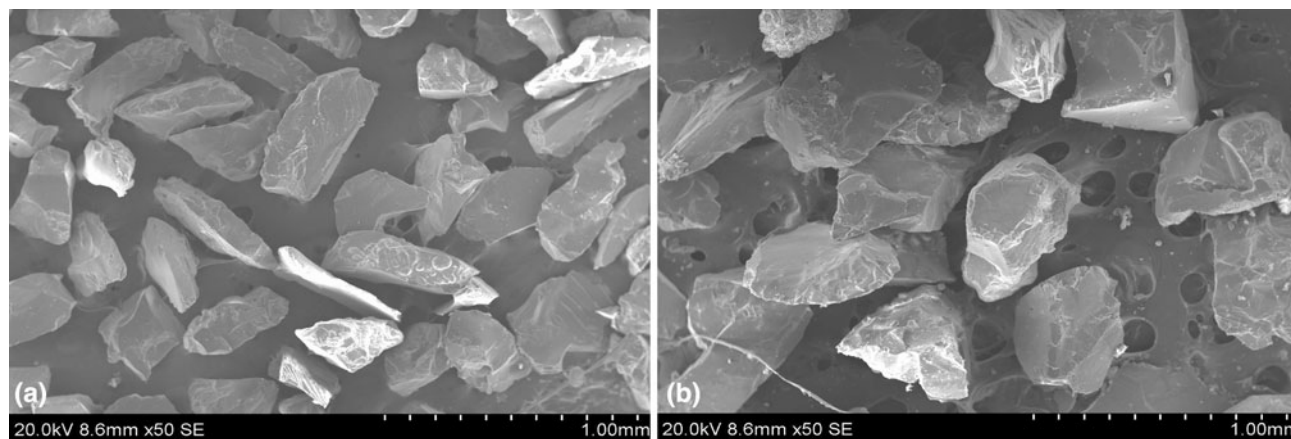


**Fig. 1** Typical SEM micrographs of (a) Alumina of 60 grit (approx. 250  $\mu\text{m}$ ) and (b) Alumina of 40 grit (approx. 420  $\mu\text{m}$ )

**Table 2** Optimized coating process parameters

Coating	Oxygen (SLPH)	Acetylene (SLPH)	Standoff dist., mm	Powder flow rate	Melting point, °C
Copper	2640	2400	140	720	1083
WC-12Co	2800	2400	165	1200	1495
Alumina	4800	1920	200	800	2049

the details of which are provided elsewhere (Ref 14). The coatings were deposited on grit-blasted mild steel substrates (30 by 30 by 5 mm) and also on grit blasted bond strength samples made from mild steel. The mild steel had a hardness of  $\text{HV } 200 \pm 20$  at 30 kg load.

The coatings were deposited using coating parameters optimized in previous studies (Ref 15, 16). The optimized parameters for the copper, WC-12Co, and alumina coatings are provided in Table 2. For the above coatings, commercially available gas atomized Cu ( $60 \pm 28 \mu\text{m}$ ; Sulzer Metco), agglomerated and sintered WC-12Co ( $28 \pm 17 \mu\text{m}$ , HC Starck) and alumina ( $13 \pm 7 \mu\text{m}$ , HC Starck) were used as the feedstock powders. The coating operations were continued until a coating of thickness  $200 \pm 25 \mu\text{m}$  was obtained in each of the three coatings.

### 2.3 Surface Roughness Measurement

The grit-blasted mild steel substrates were characterized for their average surface roughness ( $R_a$ ) and also for distance between peaks ( $R_z$ ) using Perthometer (MAHR, Germany). The surface profiles of the grit-blasted samples were also obtained using Perthometer. Similarly, subsequent to the coating deposition, the roughness ( $R_a$ ) and surface profiles of the coated surfaces were also obtained using Perthometer.

### 2.4 Bond Strength Measurement

A pin type test, which avoids the use of epoxy tape, has been utilized in the present study to evaluate the coating-substrate bond strength. The specimen and test details are

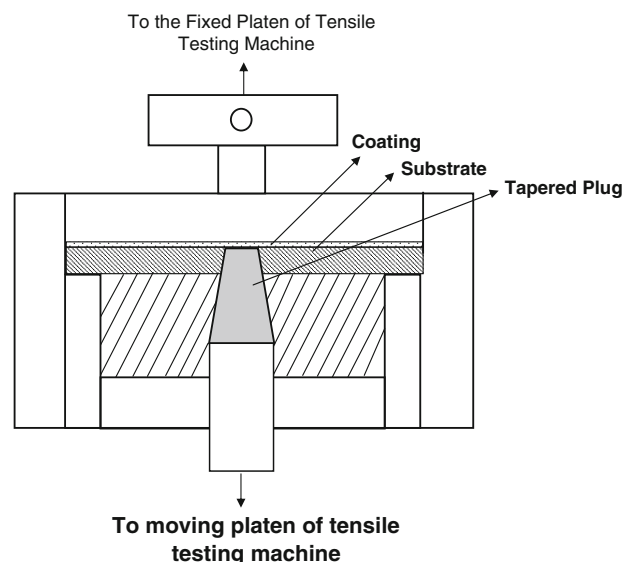


**Fig. 2** A schematic view of the experimental set up for bond strength measurement

provided in Fig. 2 and further details are provided elsewhere (Ref 17). In this method, a tapered hole is first machined through the substrate sample from its backside. A tapered plug of the substrate material is separately fabricated such that when this plug is inserted into the tapered hole in the substrate sample, it fits perfectly. Thus, the front face of the tapered plug which has a diameter of 1 mm is flush with the face of the substrate sample (see Fig. 2 for details). This assembly is then subjected to

cleaning, grit blasting on the face and subsequently coated. The assembly is then fixed in the tensile testing machine and the tapered plug is pulled down as illustrated in Fig. 2. The load/force at which the tapered plug breaks free from the coating divided by the tapered plug face area gives the tensile bond strength of the coating-substrate interface. Without exception, the fracture/separation was along the plug face-coating interface. The bond strength was obtained for all the three coatings and for each coating the bond strength was obtained as a function of grit-blasting parameters. For a given test, the experiments were repeated at least thrice and the average value has been reported. The scatter in the value of bond strength was  $\pm 15\%$ .

The extent of bonding between the coating and the substrate was also visually examined by observing the sectioned surfaces under Scanning Electron Microscope (SEM).

### 3. Results and Discussion

#### 3.1 Influence of Grit-Blasting Parameters

The mild steel substrate was grit blasted for varying time periods from 30 to 180 s, using both the coarser ( $427 \mu\text{m}$ ) and finer ( $231 \mu\text{m}$ ) alumina grits. The resulting roughness of the blasted mild steel surfaces as a function of blasting time is presented in Fig. 3 for four combinations of grit size ( $D$ ) and blasting pressure ( $P$ ). It is clear from Fig. 3 that the average roughness of the blasted surface ( $R_a$ ) does not vary substantially within increasing blasting time. However, for all the four combinations of  $P$  and  $D$ , represented by the four lines in Fig. 3, the  $R_a$  value reached a maximum value at 120 s. In view of the above, all the subsequent experiments were carried out up to a blasting time of 120 s as indicated in Table 1.

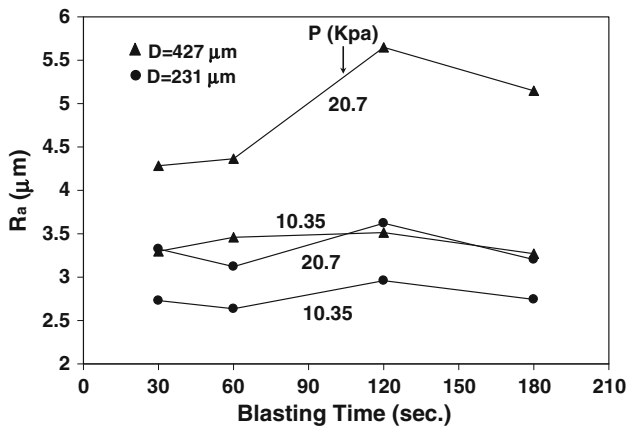


**Fig. 3** The variation of the roughness of the grit-blasted mild steel substrate ( $R_a$ ) as a function of blasting time for various combinations of blasting pressure and grit size

The influence of blasting pressure ( $P$ ) and grit diameter ( $D$ ) on the variation of  $R_a$  is presented in Fig. 4(a).  $R_a$  increases continuously with increasing blast pressure at both grit sizes. In addition, as expected, an increase in the grit size from 231 to  $427 \mu\text{m}$  increases the value of  $R_a$  at all blasting pressures. In addition to  $R_a$ , the parameter  $R_z$  which is a measure of the distance between the peaks of the blasted surface, was also measured since it is an important parameter which can influence bond strength. The correlation of the parameter  $R_z$  with  $R_a$  is presented in Fig. 4(b). An excellent correlation is observed between the two parameters implying that either  $R_a$  or  $R_z$  can be interchangeably used to assess the influence of roughness on bond strength. The actual profile of the blasted surfaces determined using Perthometer is presented in Fig. 5 for selected combinations of  $P$  and  $D$ :  $20.7 \text{ kPa}$  and  $D=427 \mu\text{m}$  (Fig. 5a);  $P=10.35 \text{ kPa}$  and  $D=427 \mu\text{m}$  (Fig. 5b);  $P=20.7 \text{ kPa}$  and  $D=231 \mu\text{m}$  (Fig. 5c); and  $P=10.35 \text{ kPa}$  and  $D=231 \mu\text{m}$  (Fig. 5d). The surface roughness profile looks nearly similar for all the four

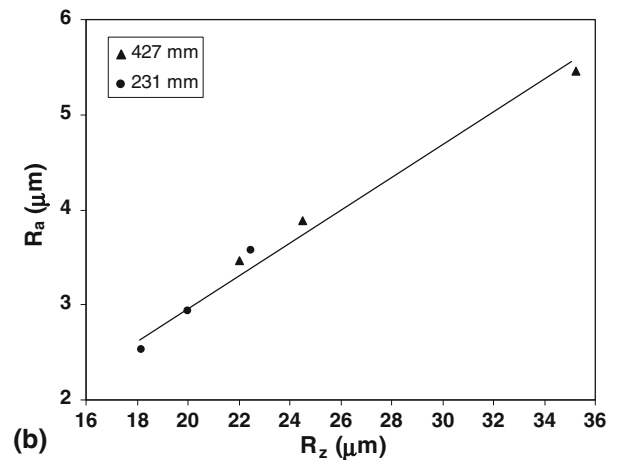
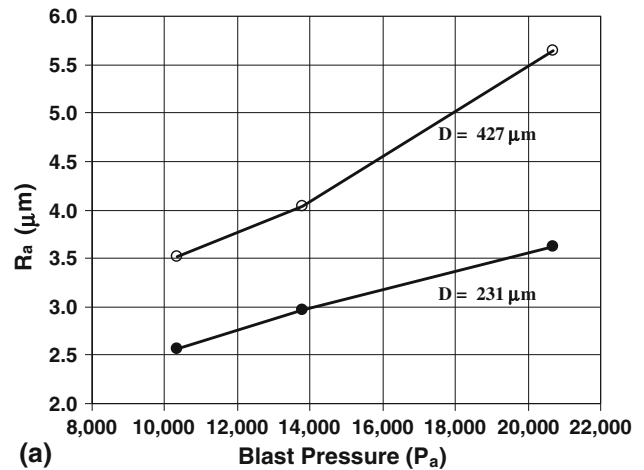


**Fig. 4** (a) The variation of the roughness of the grit-blasted mild steel substrate ( $R_a$ ) as a function of blast pressure for the two grit sizes ( $D=231$  and  $427 \mu\text{m}$ ). (b) The correlation between blasted surface parameters  $R_a$  and  $R_z$

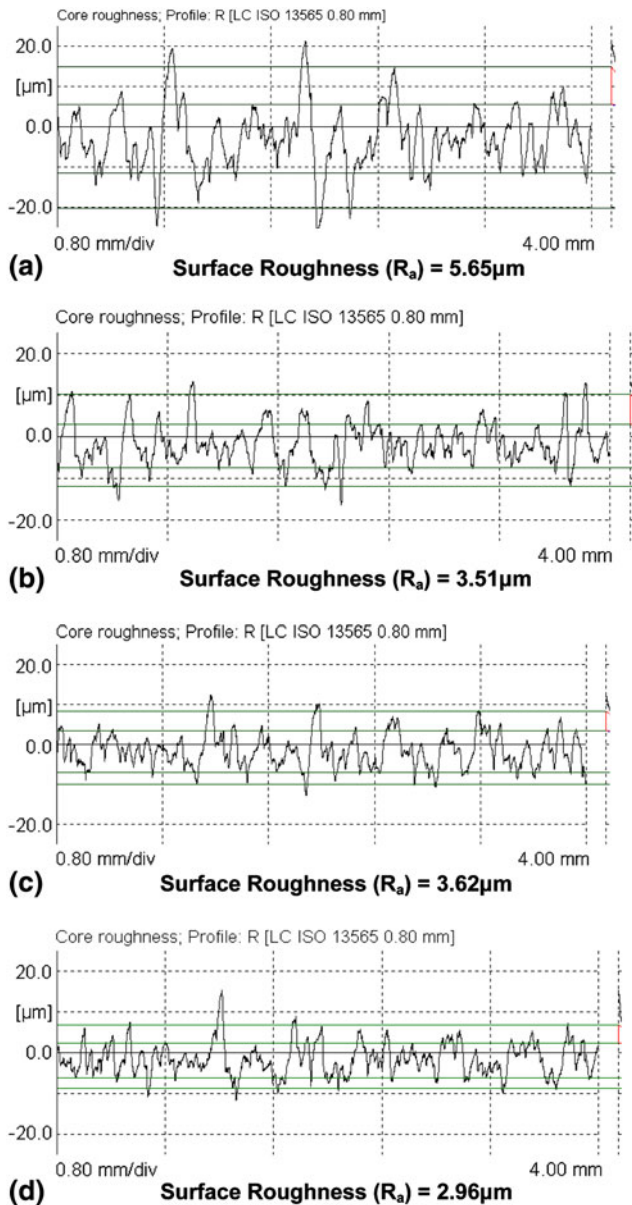


**Fig. 5** The roughness profile of the grit-blasted mild steel substrate surface (measured over a distance of 4 mm) for various combinations of grit size and blast pressure (a)  $P = 20.7$  kPa,  $D = 427$   $\mu\text{m}$ ; (b)  $P = 10.35$  kPa,  $D = 427$   $\mu\text{m}$ ; (c)  $P = 20.7$  kPa,  $D = 231$   $\mu\text{m}$ ; and (d)  $P = 10.35$  kPa,  $D = 231$   $\mu\text{m}$

combinations of blast pressure and grit diameter except for the obvious increase in the amplitude of the roughness profile with increasing  $P$  and  $D$ .

### 3.2 Grit Velocity

The experimentally measured grit velocity ( $V$ ) is a function of both the blast pressure ( $P$ ) and grit diameter ( $D$ ) as illustrated in Fig. 6. It is clear from Fig. 6 that the grit velocity increases with increasing blast pressure and decreasing grit size. An expression for the grit velocity ( $V$ ) for a given grit mass ( $m$ ) and blast pressure ( $P$ ) can be

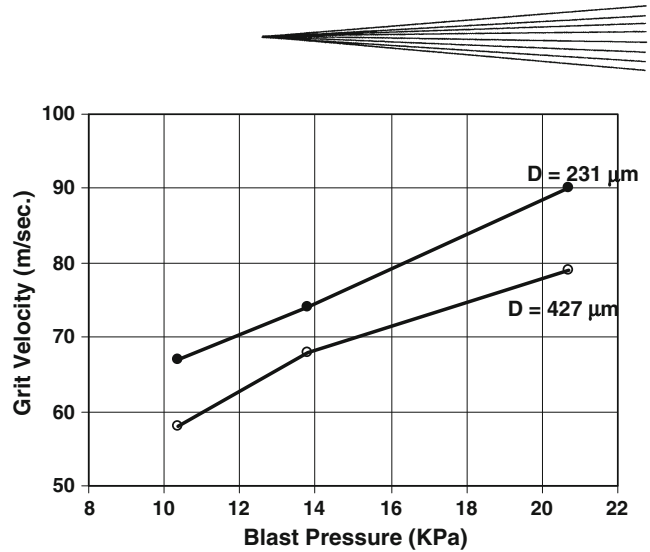


**Fig. 6** The variation of experimentally measured grit velocity as a function of blast pressure and grit size ( $D$ )

readily obtained by applying Newton's force equation to the grit. The equation of motion of the grit is then obtained as,

$$m \cdot (dV/dt) = mV \cdot (dV/dx) = P \cdot A \quad (\text{Eq 1})$$

In Eq (1),  $m$  is the mass of the grit,  $A$  is the cross-sectional area of grit which feels the pressure  $P$ ,  $t$  is the time, and  $x$  is the distance travelled by the grit. The mass and cross-sectional area of the grit are given as,

$$m = \alpha \cdot \rho \cdot D^3 \quad \text{and} \quad A = \beta \cdot D^2 \quad (\text{Eq 2})$$

In Eq (2),  $\rho$  is the density of the alumina grit and  $\alpha$  and  $\beta$  are numerical constants dependent on grit particle shape and aspect ratio. The mass of grit particle even with an asymmetric shape is the same independent of the orientation of the grit during impact. In contrast, the area of the substrate directly impacted by the grit (i.e., parameter  $A$  in Eq 1) does vary depending on the grit orientation on impact. Thus, while  $\alpha$  in Eq (2) can be treated as a constant to a good approximation, the parameter  $\beta$  in Eq (2) is expected to vary strongly with grit morphology. Since the grit shape is not the same for the alumina grits of sizes 231 and 427  $\mu\text{m}$  (see Fig. 1), it is expected that  $\beta$  in Eq (2) may not be the same for them.

Keeping the above assumptions in mind, substitution of Eq (2) in Eq (1) and solving the same gives,

$$V = (2\beta P \cdot L / \alpha \rho D)^{1/2} = C \cdot (P/D)^{1/2} \quad (\text{Eq 3})$$

In Eq (3),  $L$  is the distance travelled by the grit treated as a constant. For the alumina grits used in the present study,  $\alpha$  is expected to be a constant while  $\beta$  may be a function of grit shape and aspect ratio. As per Eq (3), grit velocity should vary as the square root of parameter  $(P/D)$  for a given grit shape and aspect ratio. In Fig. 7, the variation of grit velocity with the parameter  $(P/D)^{1/2}$  is presented. It is clear that the relationship predicted by Eq (3) is valid only for a given grit shape and aspect ratio, leading us to infer that the value of  $\beta$  in Eq (3) is not the same for grit sizes 231 and 427  $\mu\text{m}$ .

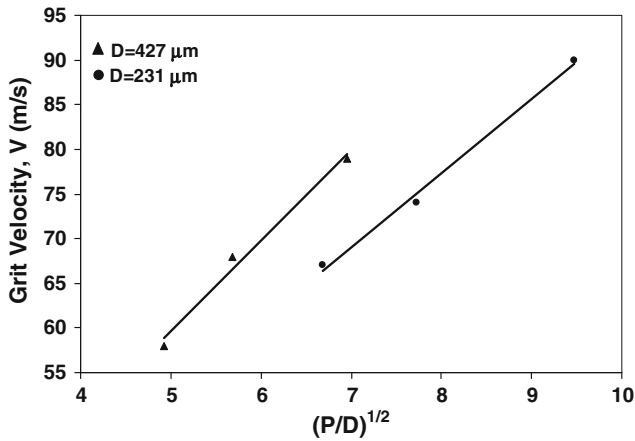


**Fig. 7** The correlation of grit velocity with the parameter  $(P/D)^{1/2}$  where  $P$  is the grit-blasting pressure and  $D$  is the grit size

The above analysis can be carried further to estimate the average surface roughness of the blasted surface (i.e.,  $R_a$ ) on the basis of grit velocity. Considering the impact of the grit (at  $90^\circ$ ) into the substrate (of hardness  $H$ ) at a velocity  $V$  as being a dynamic indentation process, a simple energy balance gives

$$\frac{1}{2} m \cdot V^2 = H \cdot V_c \quad (\text{Eq 4})$$

In Eq (4),  $V_c$  is the volume of the crater formed by the indentation process. The volume of the crater when the depth of penetration ( $d$ ) is much smaller than the grit diameter ( $D$ ) is given as,

$$V_c = (\pi/2)d^2 D \quad (\text{Eq 5})$$

Substitution of Eq (5) for  $V_c$  and Eq (2) for  $m$  in Eq (4) and also making the assumption that depth of indentation is proportional to  $R_a$  (i.e.,  $d = \gamma \cdot R_a$ ), the final expression for  $R_a$  is obtained as

$$R_a = (\alpha \cdot \rho / \pi H \gamma^2) \cdot D \cdot V. \quad (\text{Eq 6})$$

Substitution of Eq (3) for  $V$  in Eq (6) then gives,

$$R_a = \left( \sqrt{2} \alpha^{1/2} \rho^{1/2} L^{1/2} / \pi H \gamma^2 \right) \cdot (PD)^{1/2} \propto (PD)^{1/2} \quad (\text{Eq 7})$$

Thus,  $R_a$  is expected to be proportional to square root of  $PD$ . The relationship between experimentally measured roughness ( $R_a$ ) on blasted mild steel surface and the grit-blasting parameter  $(PD)^{1/2}$  is presented in Fig. 8. A good correlation is obtained indicating that Eq (7) is broadly capable of predicting surface roughness after grit blasting.

### 3.3 Roughness After Coating

The roughness ( $R_a$ ) of the mild steel surfaces coated with Cu, WC-12Co, and  $\text{Al}_2\text{O}_3$  coatings was also measured. The surface roughness profiles of the coated surfaces are presented for two extreme blasting conditions; i.e.,  $P = 10.35$  kPa and  $D = 427 \mu\text{m}$  (Fig. 9) and

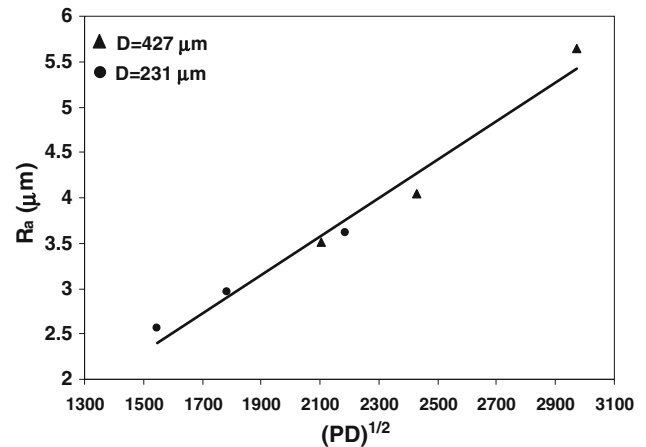


**Fig. 8** The correlation between the roughness of the grit-blasted mild steel surface ( $R_a$ ) and the parameter  $(PD)^{1/2}$

$P = 20.7$  kPa and  $D = 231 \mu\text{m}$  (Fig. 10) corresponding to the lowest (58 m/s) and highest (90 m/s) grit velocities. In both these figures (Fig. 9, 10), the roughness profile of the surface before coating is presented for reference and also the  $R_a$  value obtained for each profile is also indicated. It is clear that in the case of WC-12Co and to some extent in  $\text{Al}_2\text{O}_3$  coatings (Fig. 9c and d, 10c and d), the original surface profiles are largely retained after coating even though the number of peaks per unit length has reduced due to the powder particle impacting and spreading over the roughened substrate surface in the form of a splat. In addition, the coating roughness is higher than the substrate roughness by a factor of 20 to 80% in the case of WC-12Co and  $\text{Al}_2\text{O}_3$  coatings (Fig. 9c and d, 10c and d). In contrast, in the case of Cu coating, the roughness of the coating is dramatically higher than the original surface roughness (Fig. 9b, 10b) and more importantly only large amplitude peaks are observed unlike in the case of WC-Co and  $\text{Al}_2\text{O}_3$  coatings. The above dramatic increase with regard to the amplitude of the profile in the Cu coating is more probably due to the fact that the Cu powder used as the feedstock is larger in size ( $70 \mu\text{m}$ ) as compared to  $\text{Al}_2\text{O}_3$  and WC-Co powders. A second reason is related to the fact that the temperature of the powder particles during the detonation spray coating process is higher than the melting point of copper. Thus, unlike in the case of  $\text{Al}_2\text{O}_3$  and WC-12Co coatings, molten copper particles impact the substrate surface and spread more evenly over the roughened surface resulting in a smoother surface profile with fewer peaks.

Finally, in Fig. 11, the ratio of roughness of the coated surface ( $R_{a,c}$ ) to that of the uncoated surface ( $R_a$ ) is presented for all the three coatings as a function of  $R_a$ . It is clear that the behavior of  $\text{Al}_2\text{O}_3$  and WC-Co particles in terms of the coating process is similar since their  $R_{a,c}/R_a$  versus  $R_a$  data fall in a common line and also exhibit a trend of decreasing  $R_{a,c}/R_a$ . The data points of Cu fall separately but still in this case also  $R_{a,c}/R_a$  decreases with increasing surface roughness of the grit-blasted substrate ( $R_a$ ). In our opinion, the above difference in behavior in

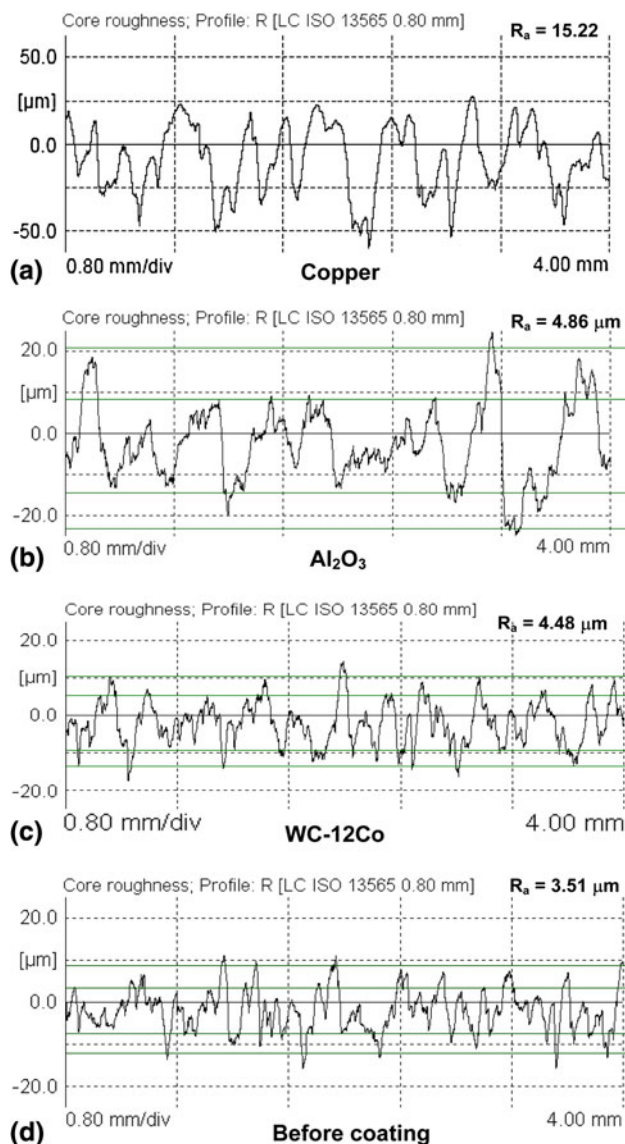


**Fig. 9** The surface roughness profile of the mild steel sample coated with (a) Copper, (b)  $\text{Al}_2\text{O}_3$ , and (c) WC-12Co for initial grit-blasting conditions of  $P=10.35$  kPa and  $D=427$   $\mu\text{m}$ . The surface roughness profile of the grit-blasted substrate without coating is provided for reference in (d)

the case of copper is mainly due to the fact that Cu particles are molten when they impact the substrate surface.

### 3.4 Bond Strength and Roughness

A traditional method to assess the quality of the bonding between the coating and the substrate is to section the sample perpendicular to the coating surface so that the coating-substrate interface can be examined visually using SEM. SEM micrographs of the sectioned surfaces are presented for Cu, WC-12Co, and  $\text{Al}_2\text{O}_3$  coatings in Fig. 12, 13, and 14 respectively. In each of these figures, the top two micrographs represent the coatings formed at the blasting pressure of 10.35 kPa while the bottom two micrographs correspond to coatings formed on the substrate grit blasted

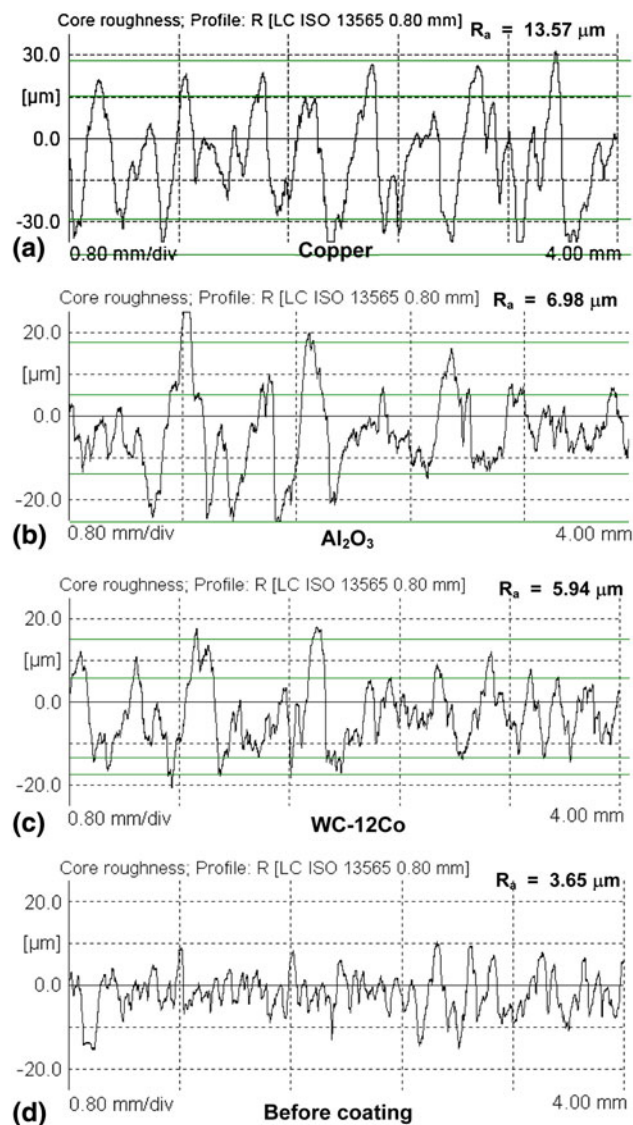


**Fig. 10** The surface roughness profile of the mild steel sample coated with (a) Copper, (b)  $\text{Al}_2\text{O}_3$ , and (c) WC-12Co for initial grit-blasting conditions of  $P=20.7$  kPa and  $D=231$   $\mu\text{m}$ . The surface roughness profile of the grit-blasted substrate without coating is provided for reference in (d)

at a pressure of 20.7 kPa. The size of the  $\text{Al}_2\text{O}_3$  grit used for blasting is also indicated in each micrograph. All the micrographs (Fig. 12 to 14) indicate the interface to be wavy (caused by roughening of substrate by grit blasting) and clean. The interface is clearly seen and is without cracks in the case of WC-Co and  $\text{Al}_2\text{O}_3$  coatings (Fig. 13 and 14). However, in the case of Cu coatings (Fig. 12), the interface is less clearly separated and also there is evidence of interface cracks. The fact that the Cu particles impact the substrate in a molten form (unlike in the case of WC-12Co and  $\text{Al}_2\text{O}_3$  coatings) is most likely to be reason for the interface cracks since solidification of the Cu droplet results in shrinkage which then induces tensile stresses at the interface between the solidifying Cu droplet and the substrate. Another aspect common to all the

coatings is that the amplitude and the wavelength of the waviness is larger for the coatings formed on substrates grit blasted with the larger  $\text{Al}_2\text{O}_3$  grit.

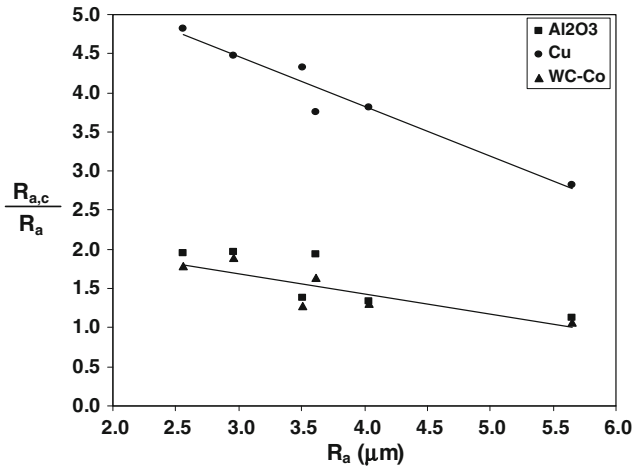


**Fig. 11** The correlation between the roughness ratio ( $R_{a,c}/R_a$ ) and the surface roughness of grit-blasted surface ( $R_a$ ) for all the three coatings

The variation of bond strength of all the three coatings with grit velocity is presented in Fig. 15. Generally, the bond strength increases with increasing blast pressure and increasing grit size. Among the coatings, WC-Co coatings have the highest bond strength values and Cu coatings the lowest. The lowest bond strengths in the case of Cu coatings is most probably related to lack of interface integrity caused by the solidification of Cu powders on impacting the substrate. The highest bond strengths observed in the WC-12Co coatings is most probably due to the fact that the Co phase is likely to melt or soften considerably at the temperatures experienced by the WC-Co particles as a whole during the DSC process. As a result, WC-Co particles are able to spread evenly aided by the fluid Co phase resulting in good bond strength. In the case of  $\text{Al}_2\text{O}_3$  coatings, there is no likelihood of fluidization or melting of the  $\text{Al}_2\text{O}_3$  particles since the temperatures experienced by these particles are substantially lower than the melting point of  $\text{Al}_2\text{O}_3$ .

The correlation between the bond strength of the coatings and the roughness of the uncoated substrate ( $R_a$ ) is illustrated in Fig. 16. The results are quite interesting since in all the three coatings, the bond strength improves from a low value to a high value beyond a roughness value

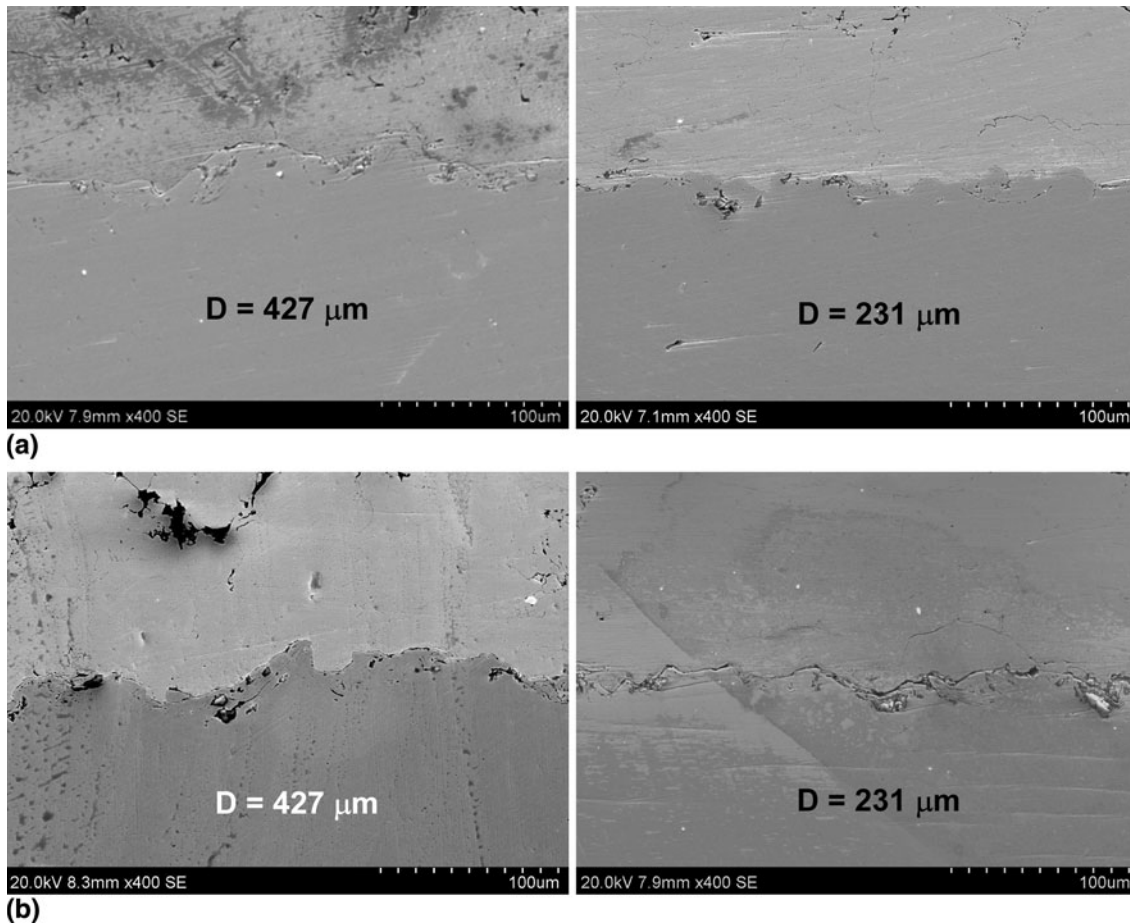


**Fig. 12** SEM micrographs of the cross section in the case of Cu coated on mild steel for blasting pressure of (a) 10.35 and (b) 20.7 kPa



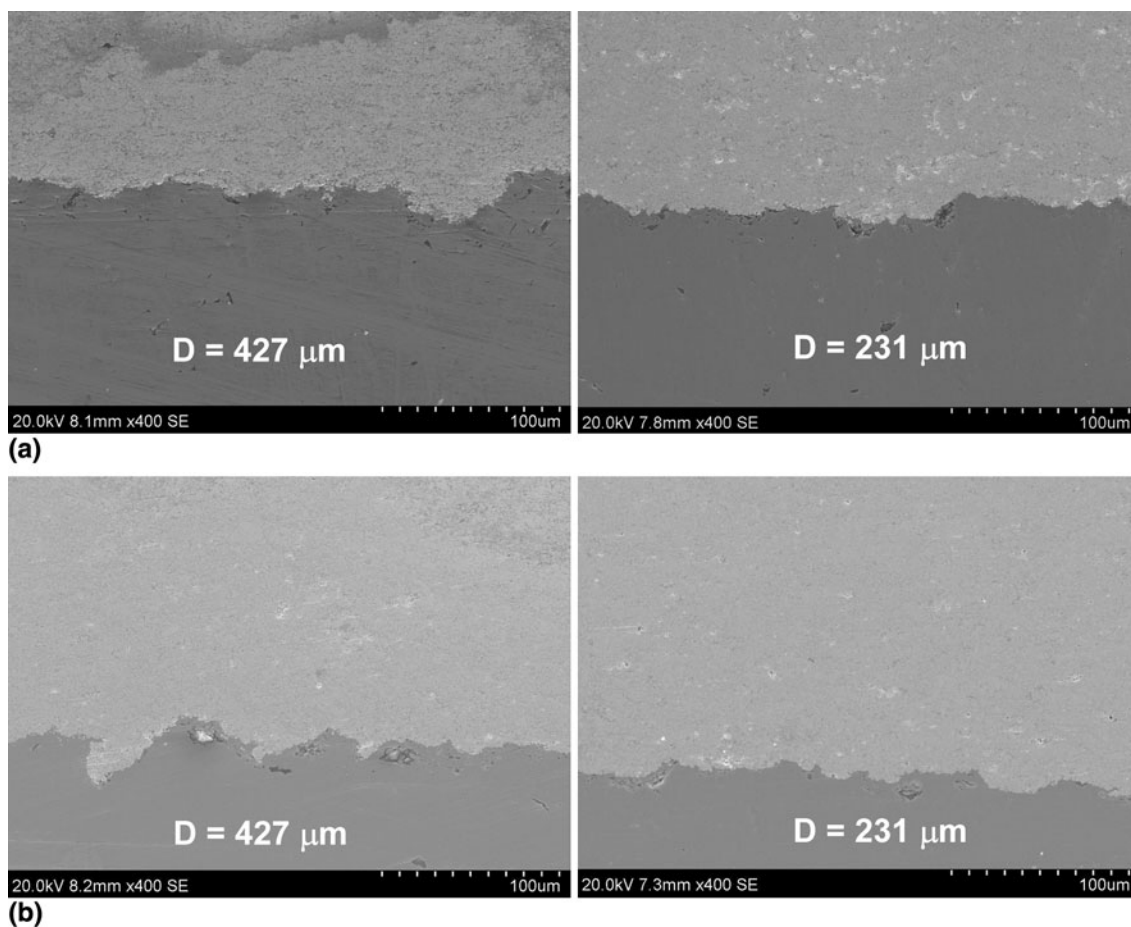


**Fig. 13** SEM micrographs of the cross section in the case of WC-Co coated on mild steel for blasting pressure of (a) 10.35 and (b) 20.7 kPa

of 3.5 to 4  $\mu\text{m}$ . Thus, it appears that a roughness ( $R_a$ ) of at least 4  $\mu\text{m}$  is necessary for obtaining the best bond strength for a given coating system and this in turn means that the alumina grit size ( $D$ ) and blast pressure ( $P$ ) should be such that the parameter  $(DP)^{1/2}$  exceeds a value of  $2200 \pm 100 \text{ Pa}^{1/2} \mu\text{m}^{1/2}$  (see Fig. 8).

Lastly, it also appears that the bond strength is intimately related to the roughness ratio ( $R_{a,c}/R_a$ ) as demonstrated in Fig. 17. All the data, for all the three coatings, fall in a band which indicates that bond strength increases substantially with decreasing roughness ratio ( $R_{a,c}/R_a$ ). The reasons behind this behavior are yet to be analyzed fully especially since there is no reason to expect the roughness of the coated surface to influence the bond strength between the blasted substrate and the coating. It is more likely that the roughness of the coated surface is an indicator of some other parameter like powder size, its flowability etc. On the basis of the present work, it can be concluded that for a given coating system, roughness of the grit-blasted substrate ( $R_a$ ) determines the magnitude of bond strength (Fig. 16). In addition, the magnitude of the bond strength of all the coatings is also strongly influenced by the roughness ratio (Fig. 17).

The above results, though interesting and new, have to be validated by carrying out experiments similar to that carried out in the present study for a larger combination of coatings and substrates. In addition, the other parameters not considered in the present study like the extent of residual grit present at the coating-substrate interface and the residual stress in the blasted surface as a function of blasting parameters may also strongly influence the bond strength. Thus, the present work represents only a preliminary effort.

#### 4. Conclusions

The major conclusions resulting from this study are as follows:

- (a) The experimentally measured grit velocity ( $V$ ) increases with decreasing grit size ( $D$ ) and increasing blast pressure ( $P$ ) and the above relationship is described as  $V \propto (P/D)^{1/2}$ .
- (b) The surface roughness ( $R_a$ ) of the grit-blasted mild steel substrate once again is a function of grit size and

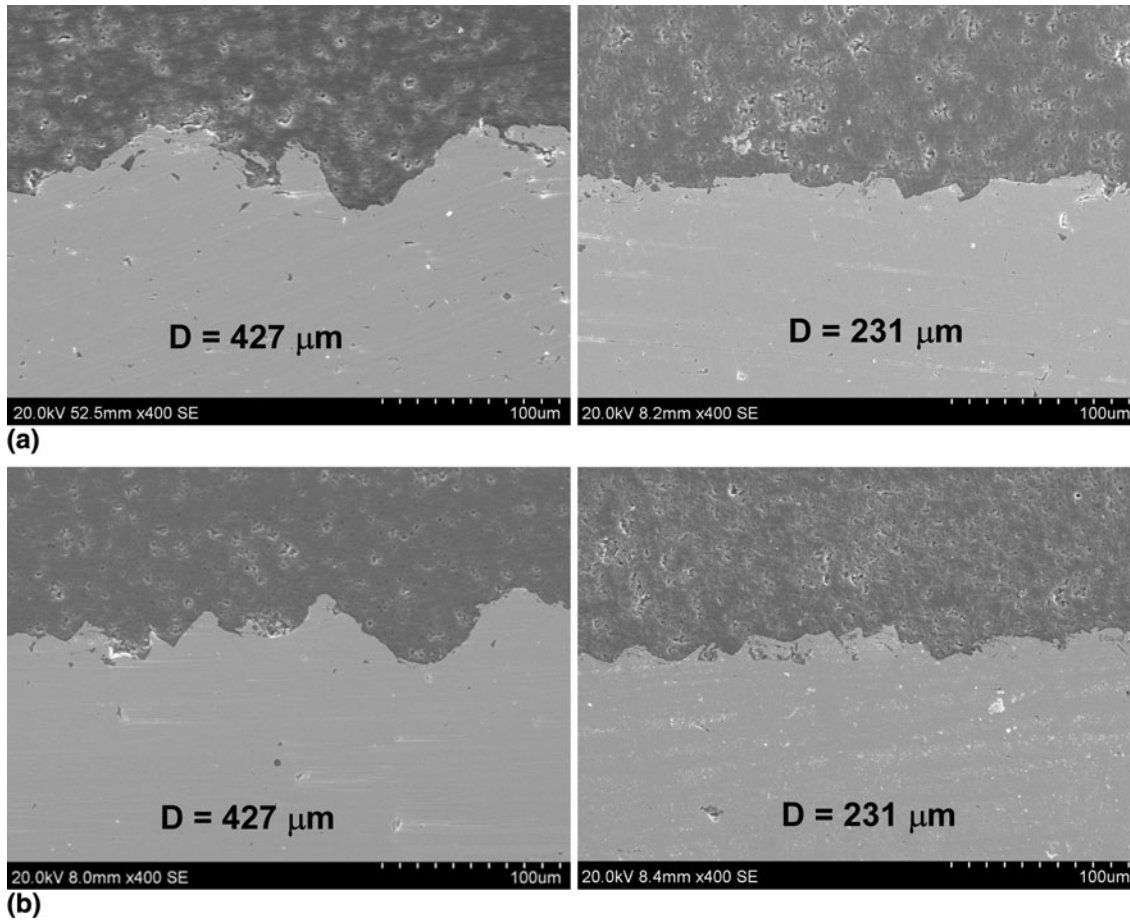


**Fig. 14** SEM micrographs of the cross section in the case of  $\text{Al}_2\text{O}_3$  coated on mild steel for blasting pressure of (a) 10.35 and (b) 20.7 kPa

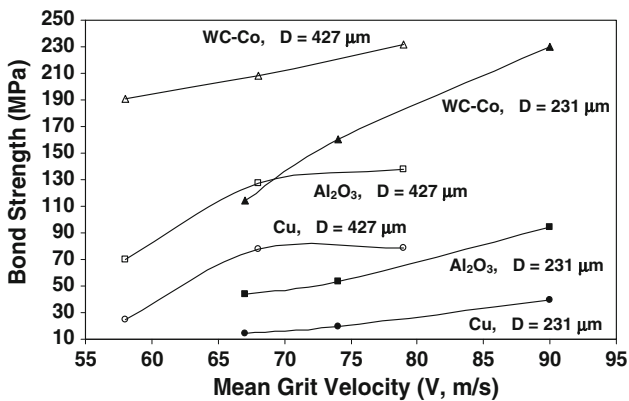


**Fig. 15** The influence of grit velocity on the tensile bond strength of Cu,  $\text{Al}_2\text{O}_3$ , and WC-Co coatings

blast pressure and the above relationship is adequately described as  $R_a \propto (P \cdot D)^{1/2}$ .

(c) The roughness of the coatings formed on the grit-blasted mild steel substrate is substantially higher than the substrate roughness in the case of copper. In the

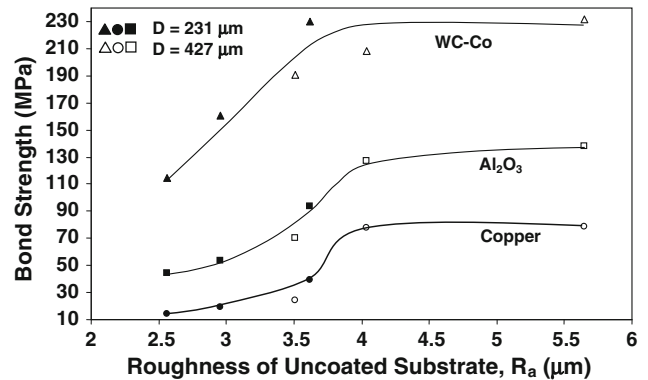


**Fig. 16** The influence of the surface roughness of grit-blasted mild steel substrate on the bond strength of the Cu,  $\text{Al}_2\text{O}_3$ , and WC-Co coatings deposited on them using detonation spray coating technique

case of  $\text{Al}_2\text{O}_3$  and WC-12Co coatings, their roughness is only marginally higher than that of the grit-blasted surface roughness.

(d) The WC-Co coatings exhibit the highest bond strength values while Cu coatings exhibit the lowest bond

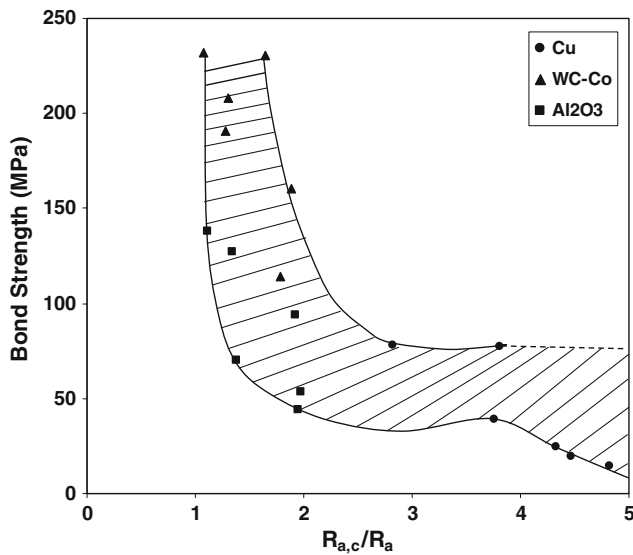
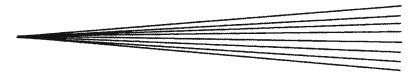


**Fig. 17** The relationship between the bond strength of the Cu, WC-Co, and Al<sub>2</sub>O<sub>3</sub> coatings and the roughness ratio ( $R_{a,c}/R_a$ )

strengths. Al<sub>2</sub>O<sub>3</sub> coatings have intermediate bond strength values.

- (e) In the case of coatings evaluated in the present study, a minimum surface roughness of 3.5 to 4  $\mu\text{m}$  has to be achieved by grit blasting with regard to the roughness of the mild steel substrate (prior to coating) in order to obtain the highest bond strength values for each of the three coatings.
- (f) There appears to be a relationship between the magnitude of the bond strength and the ratio of coating to substrate roughness with the bond strength increasing with decreasing roughness ratio.

### Acknowledgments

The authors wish to thank Director, International Advanced Research Centre for Powder Metallurgy and New Materials (ARCI), Hyderabad for granting permission to publish this paper.

### References

1. M.F. Bahbou, P. Nylén, and J. Wigren, Effect of Grit Blasting and Spraying Angle on the Adhesion Strength of a Plasma Sprayed Coating, *J. Therm. Spray Technol.*, 2006, **13**(4), p 508-514

2. J. Day, X. Huang, and N.L. Richards, Examination of a Grit Blasting Process for Thermal Spraying using Statistical Methods, *J. Therm. Spray Technol.*, 2005, **14**(4), p 471-479
3. M. Mellali, A. Grimaud, A.C. Leger, P. Fauchais, and J. Lu, Alumina Grit Blasting Parameters for Surface Preparation in the Plasma Spraying Operation, *J. Therm. Spray Technol.*, 1997, **6**(2), p 217-227
4. S. Amada, T. Hirose, and T. Senda, Quantitative Evaluation of Residual Grits Under Angled Blasting, *Surf. Coat. Technol.*, 1999, **1**, p 1-9
5. S. Amada and T. Hirose, Influence of Grit Blasting Pre-Treatment on the Adhesion Strength of Plasma Sprayed Coatings: Fractal Analysis of Roughness, *Surf. Coat. Tech.*, 1998, **102**, p 132-137
6. Z. Mohammadi, A.A. Ziaei-Moayyed, and A. Sheikh-Mehdi Mesgar, Grit Blasting of Ti-6Al-4V Alloy: Optimisation and its Effect on Adhesion Strength of Plasma Sprayed Hydroxyapatite Coatings, *J. Mater. Proc. Tech.*, 2007, **194**, p 15-23
7. T. Maruyama and T. Kobayashi, Influence of Substrate Surface Roughness on Adhesive Property of Sprayed Coating, *International Thermal Spray Conference*, May 10-12, 2004 (Osaka, Japan), ASM International, 2004, p 266-271
8. K. Poorna Chander, M. Vashista, K. Sabiruddin, S. Paul, and P.P. Bandhopadhyay, Effect of Grit Blasting on Surface Properties of Steel Substrates, *Mater. Des.*, 2009, **30**, p 2895-2902
9. M.H. Staia, E. Ramos, A. Carrasquero, A. Roman, J. Lesage, D. Chicot, and G. Mesmacque, Effect of Substrate Roughness Induced by Grit Blasting upon Adhesion of WC-17%Co Thermal Sprayed Coatings, *Thin Solid Films*, 2000, **377-378**, p 657-664
10. S. Osawa, T. Isukaichi, J. Gifu, and R. Ahmed, Influence of Substrate Properties on the Impact Resistance of WC Cermet Coatings, *International Thermal Spray Conference*, May 10-12, 2004 (Osaka, Japan), ASM International, 2004, p 492-497
11. I. Hofinger, K. Raab, J. Moller, and M. Bobeth, Effect of Substrate Surface Roughness on the Adherence of NiCrAlY Thermal Spray Coatings, *J. Therm. Spray Technol.*, 2002, **11**(3), p 387-392
12. N. Mellali, P. Fauchais, and A. Grimaud, Influence of Substrate Roughness and Temperature on Alumina coatings Adhesion-Cohesion, *Surf. Coat. Technol.*, 1996, **81**(2-3), p 275-286
13. P. Sudharshan Phani, V. Vishnukanthan, S.V. Joshi, and G. Sundararajan, Optical Diagnostics Study of Gas Particle Transport Phenomena in Cold Gas Dynamic Spraying, *J. Therm. Spray Technol.*, 2008, **17**, p 551-563
14. V. Kadyrov, M. Yakovlov, D. Sen, D. Srinivasa Rao, K.P. Rao, and A.V. Saibaba, Detonation Coating Process, *Trans. PMAI*, 1993, **20**, p 1-5
15. P. Saravanan, V. Selvarajan, D.S. Rao, S.V. Joshi, and G. Sundararajan, Influence of Process Variables on the Quality of Detonation Sprayed Alumina Coatings, *Surf. Coat. Technol.*, 2000, **123**, p 44-54
16. G. Sivakumar, L. Ramakrishna, V. Jain, D. Srinivasa Rao, G. Sundararajan, and G. Madhusudhan Reddy, The Influence of the Process Parameters on the Properties of Detonation Sprayed WC-12%Co Coatings, *Thermal Spray 2001: New Surfaces for New Millennium*, C.C. Berndt, K.A. Khor, and E.F. Lugscheider, Ed., May 28-30, 2001 (Singapore), ASM International, p 1031
17. G. Sundararajan and P. Suresh Babu, Detonation Sprayed WC-Co Coatings: Unique Aspects of their Structure and Mechanical Behaviour, *Trans. IIM*, 2009, **62**(2), p 95-103